

# An ultrasonic prospecting of shape-memory alloy behaviour under thermal charges

F. AUGEREAU, G. DESPAUX, V. GIGOT

*Laboratoire d'Analyse des Interfaces et de Nanophysique, Université Montpellier II, Place Eugène Bataillon, cc 082, 34095 Montpellier cedex 5, France*

*E-mail: augereau@lain.univ-montpa.fr*

S. LECLERCO

*Laboratoire de Mécanique et de Génie Civil, Université Montpellier II, Place Eugène Bataillon, 34095 Montpellier cedex 5, France*

---

Thermomechanical models may be produced to describe the macroscopic deformations of shape-memory alloys "educated" to be deformed with special shapes as a function of temperature. To be accurate, these models need to take into account evolution of the microstructure via homogenization theories. So, the aim of this work was to provide all available information about phase transformations occurring in the grain structures from an investigation close to the microscopic scale. In this work, we have visualized grain structures of Cu–Zn–Al duplex alloys using acoustic microscopy. Evolution of phase transformations as a function of temperature has also been followed on these acoustic images with a spatial accuracy up to few micrometres. This observation of sample surface has also enabled estimation of grain baring due to phase transformations. Using the same experimental device, "acoustic signatures" have been taken on samples in complete austenitic or martensitic forms to measure the speed of Rayleigh surface waves. Despite the use of a wide ultrasonic frequency range from 15–600 MHz, it seems that wave attenuation due to viscosity is important and disables velocity measurements by this method. Finally, using an acoustic echographic technique, we have correlated attenuation and velocity of longitudinal waves to the global phase transformation of heated samples. © 1998 Kluwer Academic Publishers

---

## 1. Introduction

Shape-memory alloys have received great attention since the early 1950s. Their first commercial success was in 1960 with the use of the properties of these metals in the engine parts of F14 US flying fighters. Since then, these special alloys have been principally used in laboratories for specific research programmes in spatial and military areas. This limited use is due to the lack of a complete knowledge of the behaviour of these alloys when they are submitted to thermal or mechanical stresses. For instance, this particular shape-modification process has to be reproducible over a long term to receive industrial applications, which is still not achieved.

Models to describe the thermomechanical behaviour of these materials are also difficult to produce. Indeed, the thermomechanical behaviour of the materials is highly sensitive to their chemical compositions and to manufacturing processes. Previous stress history and ageing mechanisms may also induce behavioural modifications.

For these reasons, further information about these phase transformations at the scale of the grain structure is needed in order to understand more completely

the origin and particularities of the large elastic deformations observed at the macroscopic scale. This information could enable the prediction of the thermomechanical behaviour of these materials from homogenization approximations of grain behaviour in order to obtain constitutive equations at a macroscopic scale.

In this context, ultrasonic techniques are suitable because they provide a non-destructive means of observing sample surface topography with a spatial resolution up to few micrometres and to detect heterogeneities inside the materials. Moreover, they produce quantitative information on small sample areas about the mechanical response of samples submitted to infinitesimal deformations.

## 2. Martensite transformations and shape-memory effect

Shape-memory alloys can be deformed up to few per cent and later recover their original shape when their temperature reaches certain limits. Basically, the particular deformation process presented by these materials is obtained from the reversible martensitic

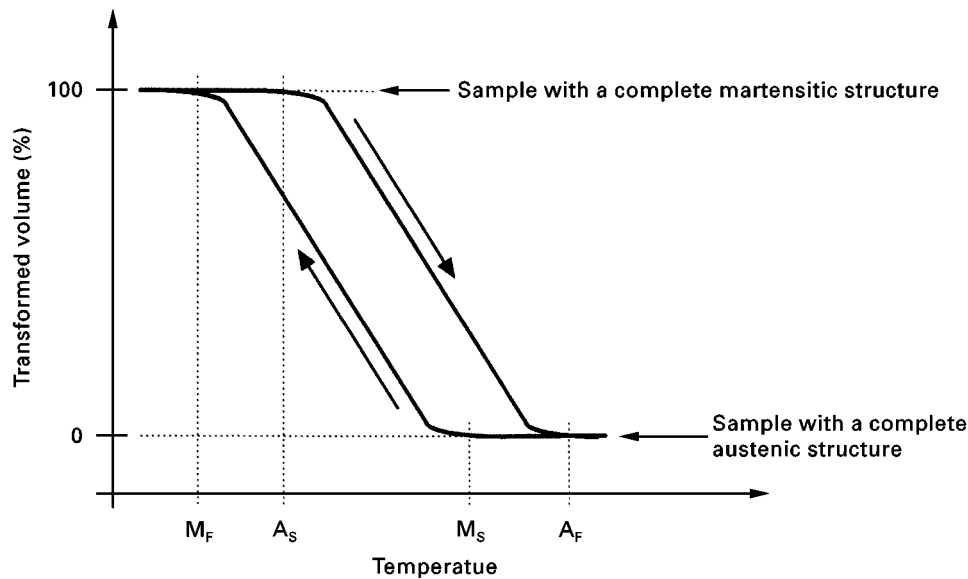


Figure 1 Theoretical temperature-dependent phase transformation diagram.  $A_S$ : temperature for the beginning of austenitic transformations in grains during heating.  $A_F$ : temperature for complete austenitic transformation in grains during sample heating.  $M_S$ : temperature for the beginning of martensitic transformations in grains during cooling.  $M_F$ : temperature for complete martensitic transformation in grains during cooling.

transformation of original austenitic grain structures. For Cu–Zn–Al alloys, these transformations appear around room temperature. This particular behaviour exists for alloys with a zinc concentration close to 38.5% and when they have been rapidly quenched in their production process. In this case, the material structure corresponds to a so-called metastable phase. In fact, with this special chemical composition, the material has a high-temperature structure also called  $\beta$ -phase, when its temperature is maintained between 900 and 850 °C. Then, under a slow cooling process, the material becomes, through a crystallization process, a duplex alloy made of  $\alpha$  and  $\beta$  phases. On the contrary, a rapid quenching limits atomic diffusion and, consequently, at room temperature the material retains its high-temperature material structure. This phase is stable but does not conform to equilibrium diagrams with respect to its chemical composition.

The martensitic transformation of this so-called metastable phase generates large deformation and is responsible for the shape-memory effect of these specific Cu–Zn–Al alloys [1]. This deformation mechanism may be induced by temperature variations or by mechanical loading. From a specific education process, it is possible to create these phase transformations always along the same specific directions. Thus, each temperature variation around the phase transformation limits produces a reproducible and reversible deformation: this corresponds to the shape-memory effect of these materials (see Fig. 1). This behaviour may also be observed with respect to the average percentage of the sample volume which is composed of martensitic structures for any given temperature.

At the macroscopic scale, this microstructure evolution due to phase transformation induces the deformation of the whole sample. In fact, much work has been done to describe theoretically this thermomechanical behaviour by special constitutive equations, taking

into account thermodynamic and mechanical considerations [2].

Austenitic and martensitic structures correspond, respectively, to a face-centred cubic  $\alpha$  phase and to a body-centred cubic  $\beta$  one. They have exactly the same chemical constitution, but, because of their different crystallographic structure, they do not exhibit the same mechanical behaviour. Previous mechanical tests have established that austenitic structures start to deform plastically at lower stress than the martensitic one [3].

### 3. Material property investigation by echography and acoustic microscopy

These techniques are based on measurement of propagation conditions of ultrasounds inside materials defined by their velocity and attenuation. These parameters depend on the samples' mechanical properties and also on their internal structure. In fact, they characterise the materials' response to small amplitude vibrations.

#### 3.1. Echography

In echographic techniques, velocity measurements are performed with plane acoustic sensors by recording the propagation time of a short ultrasonic pulse through the sample thickness. Attenuation is measured as the amplitude variation of the acoustic wave between its emission time level and after propagation inside sample.

In this work, the same sensor generates the acoustic burst and records the reflected signal amplitude after a double propagation through the sample thickness (see Fig. 2a, for explicit measurement configuration). The ultrasonic frequency used for this investigation is generally contained in the megacycle range. Time and amplitude measurements are simply done using

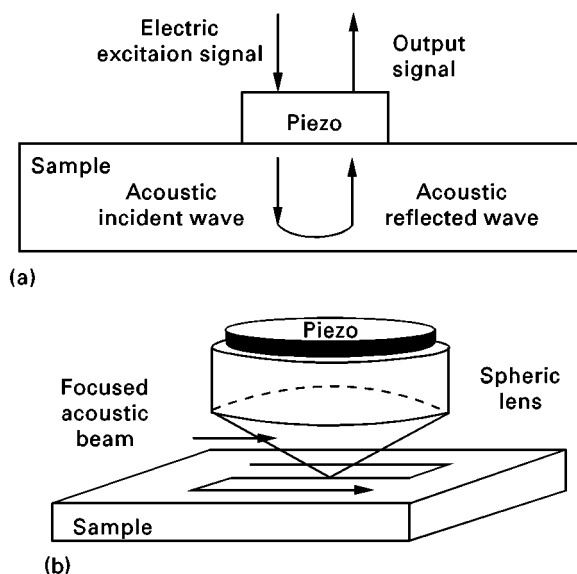


Figure 2 (a) Echographic and (b) acoustic signature measurement configuration.

voltage and time markers on an oscilloscope. The accuracy of velocity measurement by this method is around 1%.

### 3.2. Acoustic microscopy

The echographic technique cannot produce an accurate image of the material structure because the diameter of the acoustic sensor emission surface is around 5 mm. To obtain a sharper acoustic investigation of materials, acoustic microscopes use a spherical acoustic lens to focus a plane acoustic wave. At the focal length, acoustic energy is confined in a few micrometres large area according to diffraction rules. Acoustic images are then built by recording the amplitude of the focused wave reflected part and by moving the acoustic lens parallel to surface sample with a sweeping movement (see Fig. 2b). On these images, amplitude is digitized and coded on a grey scale, in which black corresponds to the smallest signal level and white to the largest one. Owing to the high attenuation level for ultrasounds in gas, a coupling fluid (water) is used to ensure an efficient propagation of acoustic waves between sensor and sample [4].

The contrast in the acoustic images has two main origins which are sample topography and mechanical properties variations from one place to another. Both effects may be present simultaneously. Mechanical properties variations correspond at the microscopic scale to differences in the material crystallographic orientation.

### 3.3. Mechanical properties investigation by acoustic velocity measurement

Ultrasonic sensors work in the megacycle range and they induce very small strains inside materials during wave propagation. Thus, it is generally admitted that a materials' mechanical behaviour may be predicted at a macroscopic scale by linear elastic theory. From this

model, elastic parameters such as Lamé constants for isotropic materials may be related to sample density and to propagation velocities of pure longitudinal and transverse waves in this material [5].

To link acoustic velocities to the signal recorded by the focused acoustic lens, a theoretical reflectance power  $R(\theta)$  is used to describe reflection conditions of acoustic waves propagating through a liquid medium towards a solid one, as function of the incident angle,  $\theta$ . Taking into account the lens sphericity, the modulus of the integral of  $R(\theta)$  from  $0^\circ$  to the lens opening aperture gives the signal amplitude measured by the sensor after reflection on sample surface for any given material. This function depends on density and also on longitudinal and transverse wave velocities of the material. Contrasts on acoustic images display these modifications of  $R(\theta)$  induced by elastic property variations over the sample surface.

By acoustic microscopy, the velocity of surface waves can be measured from the interference pattern present on "acoustic signatures". Indeed, when the amplitude of the reflected acoustic wave is recorded as a function of distance between the sample and the sensor, the resulting curve shows damped oscillations due to the phase delay between different specific waves and attenuation of acoustic waves inside the materials [6]. From the period of these oscillations measured by fast Fourier transform, surface-wave velocity may be calculated with an accuracy close to 1‰ and linked to longitudinal and transverse velocities. For this reason, the acoustic signature technique plays an important part for material property evaluation.

## 4. Acoustic observation of austenitic and martensitic structures

Cu–Zn–Al samples have been studied with an acoustic microscope to display the various metallurgical phases and their spatial distribution over the surface of this alloy.

### 4.1. Austenitic structures

When Cu–Zn–Al alloys are polished and maintained at a temperature higher than the austenitic limit,  $A_F$  (see Fig. 1), the sample surface appears to be uniform by classic optical investigation. However, under the same experimental conditions, acoustic images show the presence of homogeneous structures with an average diameter of 1 mm. The Fig. 3 shows an acoustic image realized with a 130 MHz acoustic lens at  $30^\circ\text{C}$ . All the grains do not have the same grey level. This indicates that the conditions of ultrasonic wave reflection differ from one structure to another, which corresponds to different mechanical properties. This underlines the high sensitivity level of acoustic techniques for the detection of material structure differences.

### 4.2. Martensitic structures

Martensitic structures appear on acoustic images as sharp striped lines inside austenite grains (see Fig. 4).

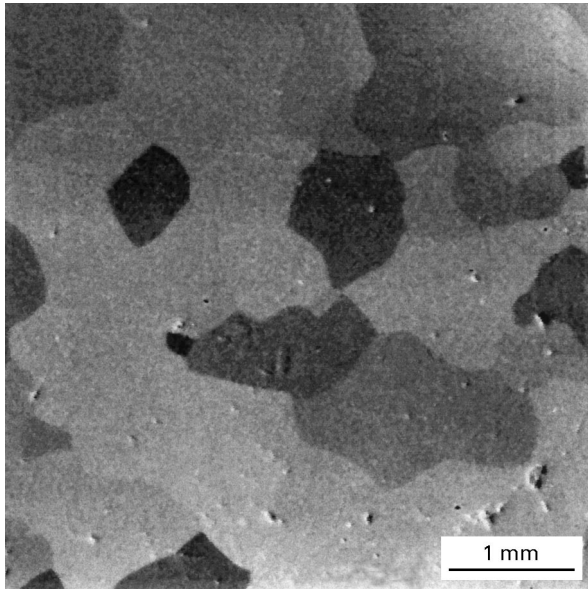


Figure 3 Austenitic grains in Cu–Zn–Al alloy observed by acoustic microscopy at 30 °C.

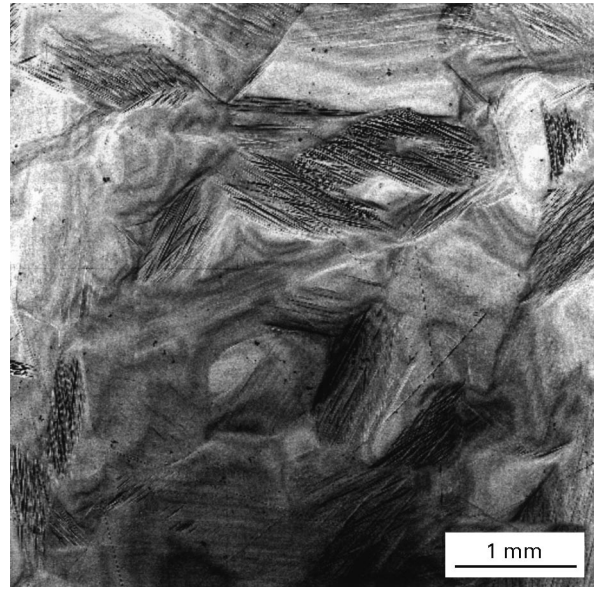


Figure 5 Visualization of grain barring by acoustic microscopy from a fringe pattern.

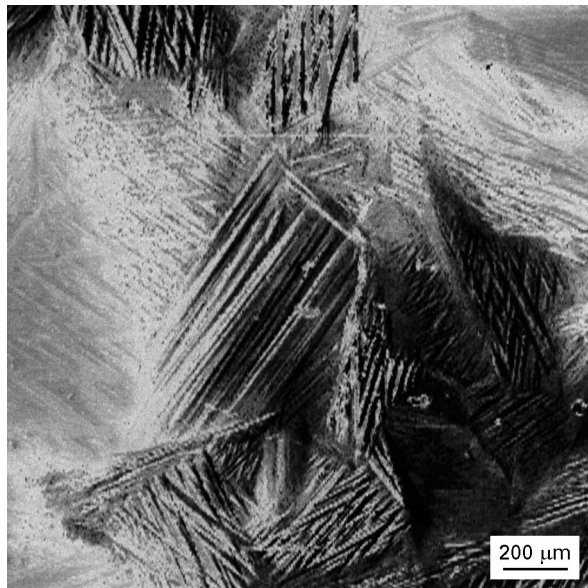


Figure 4 Martensitic structures in Cu–Zn–Al alloy observed by acoustic microscopy at 18.5 °C.

This image is realized with a 130 MHz acoustic lens at 18 °C.

Optical observation reveals the same patterns. Nevertheless, we may also observe and measure the grain barring level by acoustic microscopy. This technique is highly sensitive to sample topography and is also perturbed by any planetary mismatch between sample and sensor. For example, when acoustic images are performed on a uniform glass sample inclined by few degrees in one direction, a periodic succession of contrast fringes is present and is oriented perpendicular to the sample slope direction. These patterns correspond to the same interference process present in acoustic signatures. Their period is equal to the half-wavelength in the coupling fluid. This feature of acoustic imaging is used to measure grain barring in

polycrystalline material when the average parallelism mismatch between the samples surface and the acoustic lens is kept sufficiently small.

For example, Fig. 5 shows an acoustic image realized at 600 MHz of the surface of a Cu–Zn–Al alloy at 18 °C. As previously (see Fig. 4), martensitic structures are present inside the austenitic grains but an additional succession of contrast fringes is superimposed.

Our acoustic microscope enables estimation of the propagation time of the incident acoustic beam towards the sample surface from the visualization on an oscilloscope of the amplitude of the reflected signals on a time scale. These time measurements are less accurate than phase ones by fringe observation, but they do confirm that the fringe period in Fig. 5 corresponds to an average extra defocusing close to 2.5 μm. Thus, from contrast fringes, grain barring may be measured on acoustic images, which seems more difficult to achieve with optical techniques.

With a 130 MHz ultrasonic focused lens, the spatial resolution available is close to 10 μm, from diffraction studies (Rayleigh criteria). Martensitic structures are visualized as a succession of black to white lines. Images of the same martensitic structures realized by scanning electron microscopy have shown us that, from one striped line to another, topographical variations are less than a micrometre. Consequently, the contrast variations of these austenite structures on acoustic images at this frequency are mainly due to different mechanical properties and not to topography.

#### 4.3. Phase transformation observation under thermal loading by acoustic imaging

In the second part of this experimental study, we have demonstrated the ability of acoustic microscopy to follow gradual evolutions of austenitic and martensitic

grains as a function of temperature. From these observations, orientations and shapes of martensitic structures could be analysed for a better understanding of the memory effect in these alloys.

To follow the phase transformations process, the sample was submerged in a temperature regulated water tank. Then, acoustic images were taken at various temperatures to observe step-by-step the gradual transformations of grains.

This study of phase transformations may also be performed for mechanical loads applied to memory alloy samples using a specific experimental tool we built. This device stresses samples and enables acoustic imaging of material under stress at different temperatures.

## 5. Measurement of ultrasonic wave velocity and attenuation in Cu–Zn–Al alloys

Measurements of ultrasonic propagation parameters enable detection of mechanical properties variations. This information may be obtained from different parts of the sample surface by acoustic signature and echography.

### 5.1. Acoustic signatures

For some materials, the interference process at the origin of acoustic signatures does not exist, which precludes any velocity measurement. This occurs when the acoustic focused lens cannot propagate surface waves in this material, due to an incorrect incident angle or when the surface waves are too heavily attenuated inside the samples [6]. In this work, we did not succeed in measuring the velocity for these shape-memory alloys, because no oscillations were present on the acoustic signatures. However, if we suppose that Cu–Zn–Al alloys have acoustic properties close to those of brass (Cu 70%, Zn 30%:  $V_L = 4400 \text{ m s}^{-1}$ ,  $V_R = 1960 \text{ m s}^{-1}$  from [6]), this indicates that  $V_R$  and  $V_L$  would have been detected by acoustic signatures with the  $50^\circ$  opening aperture lenses we used.

Wave attenuation is generally linked to viscous mechanical behaviour or to microscopic structure discontinuities such as dislocations, cracks or grain boundaries, which produce wave scattering during wave propagation. To study the origin of wave attenuation in these shape-memory alloys, we performed acoustic signature measurements on a large frequency scale from 15–600 MHz. Attenuation by a scattering process is dominant when the acoustic wavelength is equal to or lower than the sample inhomogeneity dimensions. On acoustic images, grains in these alloys are about  $500 \mu\text{m}$  in size. So, with a 600 MHz acoustic lens, the grain-boundaries effect vanishes when acoustic signatures are taken at the grain centre. Experimentally, these acoustic signatures on grains in the austenitic or martensitic state present no oscillations at 600 MHz.

In order to decrease perturbations induced by microscopic defaults on acoustic wave propagation, measurements were also taken at 15 MHz, but with no

better result. All these tests indicate that the high attenuation level is not due to the presence of heterogeneities in these alloys.

Next, we used a  $50 \mu\text{m}$  thick Cu–Zn–Al alloy layer stuck to a glass substrate to improve wave propagation conditions. At low frequency, surface wave propagation should be mainly sensitive to mechanical properties of the glass substrate and, consequently, acoustic signatures should become measurable. We used a 15 MHz acoustic lens and despite the thinness of this Cu–Zn–Al layer compared to the acoustic wavelength, no oscillations were present on the acoustic signatures.

Thus, this study demonstrates that the strong attenuating effect of this material for surface wave propagation is mostly due to a viscous mechanical behaviour rather than to a scattering process produced by a specific microstructure.

### 5.2. Echographic measurement

We used a plane acoustic sensor which creates longitudinal waves inside the materials. These special waves have the particularity to generate only compression–traction displacements inside materials. The measurement configuration is described in Fig. 2b. In order to obtain a measurable reflection echo after a double propagation through the sample thickness, a low-frequency sensor was used with a 4 MHz working frequency. The active surface of this sensor for acoustic emission and detection is around  $0.5 \text{ cm}^2$ , which indicates that each measurement will concern several grains of the material structure. With this device, propagation time and maximum amplitude of the first reflection echo are measured as function of the average temperature of the water vessel containing the sample. Corresponding variations are presented in Figs 6 and 7. Temperature was measured with a  $0.1^\circ\text{C}$  precision thermocouple. With this simple measurement device, time delay and voltage were measured with error percentages close to 0.5% and 2%, respectively.

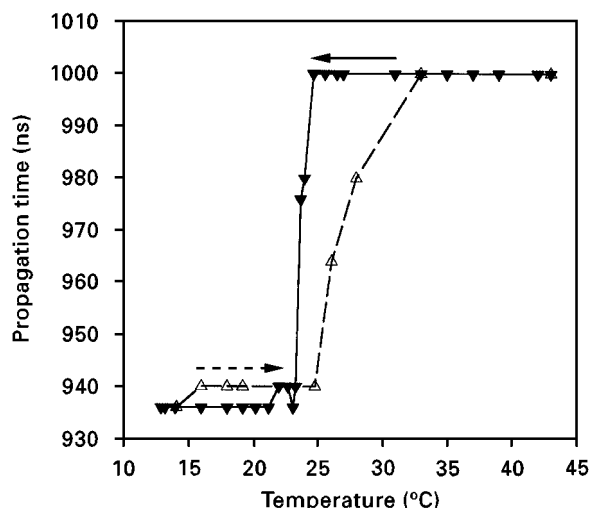


Figure 6 Effect of temperature on propagation time of a 4 MHz longitudinal wave after a double propagation through the thickness of a Cu–Zn–Al alloy sample: (▼) cooling, (△) heating.

TABLE I Limiting temperatures for phase transformation deduced from propagation time measurement by ultrasonic echography

	End of austenitic transformation, $A_f$	Start of austenitic transformation, $A_s$	End of martensitic transformation, $M_f$	Start of austenitic transformation, $M_s$
Temperature (°C)	$28 < A_f < 33$	24.8	23.3	24.7

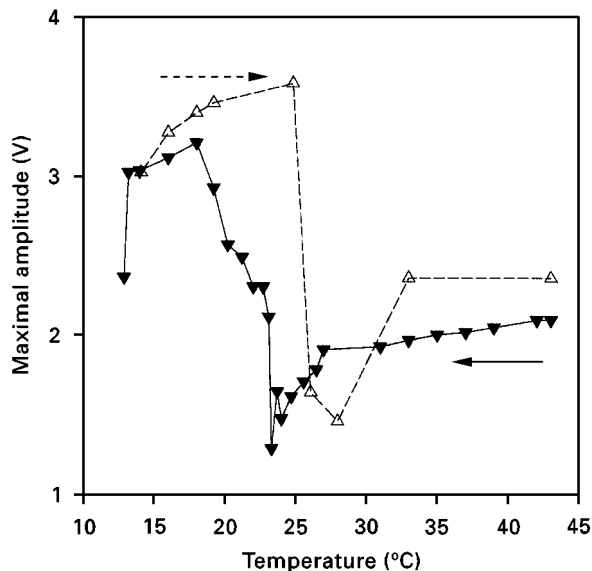


Figure 7 Effect of temperature on the echo amplitude of a 4 MHz longitudinal wave after a double propagation through the thickness of a Cu–Zn–Al alloy sample: (▼) cooling, (△) heating.

First, these experimental results demonstrate the sensitivity of this technique to the average level of phase transformation as temperature changes. Indeed, phase transformations correspond to sudden echo amplitude and propagation time variations. During successive cooling and heating procedures, echo amplitude and propagation time variations present an hysteresis phenomenon comparable to the theoretical graph of transformed volume versus temperature (see Fig. 1). Propagation time seems to be the most reliable parameter to determine austenitic and martensitic temperature limits during the cooling or heating process (see Table I).

In the temperature range between 10 and 35 °C, the thickness variation is less than 10 µm for a 2 mm thick sample. So, if this parameter is considered to be unchanged with temperature, the longitudinal velocity,  $V_L$ , of this alloy is estimated to be 4000 ms<sup>-1</sup> for a totally austenitic state compared with a value of 4250 ms<sup>-1</sup> in the completely martensitic state. The minimum relative error for this velocity measurement is estimated to be 0.4%.

## 6. Conclusion

Using acoustic microscopy, austenitic structures may be observed on the surface of a Cu–Zn–Al sample by acoustic imaging with a spatial resolution of up to a few micrometres. Contrasts present on these

acoustic images are induced by different wave reflection conditions which are directly linked to mechanical properties variations. Orientations and shapes of martensitic structures are also observable on the Cu–Zn–Al alloys. Moreover, this technique provides the additional capability to measure, accurately, grain baring on acoustic images from fringe observation.

In this experimental work, we have also demonstrated that acoustic microscopy is a suitable means to observe the gradual phase transformation process induced by a thermal load applied to these shape-memory alloys.

In a first attempt to correlate the phase transformation state to ultrasonic wave velocity, we used the acoustic signature technique. Unfortunately, the high attenuation level of the Cu–Zn–Al alloy, due to its viscosity, prevents the actual measurement of surface wave velocity by this technique.

Finally, this work demonstrated the effective sensitivity of longitudinal wave propagation conditions to phase transformations in a Cu–Zn–Al shape-memory alloy by echographic measurements. Indeed, from velocity and attenuation measurements, this technique has enabled a global estimation of the state of metallurgical transformation. Thus, austenitic and martensitic limit temperatures may be accurately measured without the need for special sample preparation.

## Acknowledgements

We thank Professors A. Chrysochoos and R. Peyroux, LMGC staff (University of Montpellier II, France), for provision of the shape-memory alloys, and for their helpful comments.

## References

1. E. PATOOR and M. BERVEILLER, in "Technologie des alliages à mémoire de forme" (Editions Hermès, Paris, 1994) (in French) pp. 48–53.
2. A. CHRYSOCHOOS, M. LÖBEL and O. MAISONNEUVE, *C. R. Acad. Sci. Paris* **320** Série Iib (1995) 217 (in French).
3. R. W. K. HONEYCOMBE and W. BOAS, *I.I. Metals*, Vol. 73, p. 443 (1947).
4. R. J. M. DA FONSECA, L. FERDJ-ALLAH, G. DESPAUX, A. BOUDOUR, L. ROBERT and J. ATTAL, *Adv. Mater.* **5** (1993) 508.
5. B. A. AULD, "Acoustic fields and waves in solids", Vol. I (Wiley-Interscience Publication, John Wiley & Sons, New York, London, Sydney, Toronto, 1973).
6. A. BRIGGS, "Acoustic Microscopy" (Clarendon Press, Oxford, 1992).

Received 16 October 1997  
and accepted 15 May 1998